

## Structural Properties of Island Films of Indium on Si(111) and the Sputter-Etching Profile

Shigeru BABA<sup>\*1</sup>, Makoto IOZAKI<sup>\*2</sup>, Shogo SATO<sup>\*3</sup>, Takeo NAKANO<sup>\*4</sup>

**ABSTRACT** : Indium films of mass-thickness from 20 to 180 nm were deposited on Si(111) substrate. Films consisted of cap-shaped islands. The morphology and the surface coverage were studied with atomic force microscopy and the secondary electron microscope (SEM). Atomistic composition of the surface was measured with X-ray photoelectron spectroscopy (XPS). The surface composition of indium was found greater than the apparent coverage of islands. The island films were sputter-etched with an ion beam of Ar<sup>+</sup>. The change in the surface composition with sputtering time, which was usually called as a depth profile, was found to have a common profile as a function of the sputtering time divided by the film thickness. This universal nature can be explained by assuming that the silicon surface is covered with indium islands of the same shape and that the similarity in shape is maintained during the sputtering. The morphological change caused by the sputtering was also studied with SEM when the surface composition by XPS became 0.71, 0.50 and 0.25, respectively. It was observed that islands shrank in size while keeping the similarity in shape.

PACS number: 61.05.Np, 68.43.Hn, 68.49.-h, 68.55.-a

**Keywords** : Depth-profile, Island structure, Sputtering yield, Indium

(Received April 7, 2011)

### 1. Introduction

The initial stage of film growth crucially influences the performance of technological devices such as sensors, catalysts, optical and electronic applications, and the nucleation and growth of thin metal films has been investigated for long years with the development of measurement techniques.<sup>1</sup> The morphology of thin films varies not only with the combination of film and substrate materials but also with the deposition condition.<sup>2</sup> Under near thermal equilibrium, especially for low melting point metals, either mode of Volmer-Weber, Stransky-Krastanov, or Frank-van der Merwe appears according as the total energy of the surface, the interface and the volume is minimized.

We have been interested in Cu-In alloy films, and investigated the surface roughness and electrical

properties. A mixture of intermetallic compounds such as CuIn<sub>2</sub> could be observed, and the relation between the roughness and the composition has been reported.<sup>3,4</sup> After annealing the layered Cu-In films, islands of indium are formed on the surface as a result of the segregation of indium when the averaged composition exceeds 65 at.%.

The technique of surface spectroscopy such as Auger electrons and X-ray excited photoelectrons has been applied successfully to the classification of the film growth mode<sup>5,6</sup> though a fundamental research for more sensitive methods has been exploited.<sup>7</sup> For example, when the signal intensity of the film material increases linearly with the deposited amount, deposited atoms are considered to be on the way of top-layer formation on the lower completed layers.

Observation of the change in elemental composition by sputter-etching has been widely used as the first tool to analyze the sub-surface structure,<sup>8</sup> and the data is called a depth profile. If a proper etching model is employed, we can acquire information on the film structure by analyzing the data.<sup>9</sup>

<sup>\*1</sup> : Professor, Department of Materials and Life Science, Science and Technology, Seikei University. (baba@st.seikei.ac.jp)

<sup>\*2</sup> : Undergraduate Student, Seikei University.

<sup>\*3</sup> : Graduate student, Seikei University. NEC Engineering Ltd (present affiliation).

<sup>\*4</sup> : Assistant Professor, Seikei University.

In our previous paper, pure indium was deposited on a silicon surface to study the island growth, and a common profile that the depth profile was independent of the film thickness was found. To explain the result, we proposed a model that the sputtered islands were similar in the shape.<sup>10</sup> There were some backgrounds that support this assumption. Indium atoms easily migrate on the surface at room temperature because the melting point of indium is 156.6°C, and they tend to cover the silicon surface because the surface energy of indium is lower than that of silicon. Furthermore indium does not form any intermetallic phases with silicon as a simple binary alloy system.<sup>11</sup> In the present paper, the film structure of indium and the change caused by the sputter-etching are examined in detail.

## 2. Experiments

Substrates of  $10 \times 25 \text{ mm}^2$  were cut out from the wafer of n-type Si(111),  $\rho = 0.1 \text{ } \Omega\text{cm}$ , and then the oxide layer was etched off in a dilute HF solution. Indium films were deposited in a vacuum system (EBV-6CH, ULVAC). The chamber was pumped down by an oil-diffusion pump with a liquid  $\text{N}_2$  trap to a pressure of less than  $2 \times 10^{-4} \text{ Pa}$  during deposition. The substrates were heated to  $150^\circ\text{C}$  for 1 hour in vacuum and then kept at  $80^\circ\text{C}$  during the deposition. A series of film thicknesses ranged from 20 to 180 nm were deposited from the molybdenum boat. The deposition rate was monitored with a quartz deposition controller (XTC, INFICON Inc.) and was kept at about 0.2 nm/s.

The morphology of indium islands was first studied with an atomic force microscope (AFM: Quesant Resolver). Surface areas of  $20 \times 20 \text{ } \mu\text{m}^2$  were scanned at a z-resolution of 0.1 nm, and the images showed a densely-arranged island structure on the surface.<sup>10</sup> The island diameter was about  $0.5 \text{ } \mu\text{m}$  for films of 60 nm thick for example. Alternative observation of the surface was performed at a higher resolution by a scanning electron microscope (SEM: JSM-6510, JEOL). The surface images were taken at a beam acceleration voltage of 15 kV with the spot size of 40 nm.

The SEM images of indium films of 30, 60, 90 and 120 nm-thick are given in Fig. 1. The magnification

of Fig. 1 (b), (c) and (d) is the same and the scale bars indicate  $1 \text{ } \mu\text{m}$ , while that of Fig. 1 (a) is 2.5 times as large as the rest. Though the island size shows a distribution in each image, all images can be assumed to be similar, and the average size and the dispersion increase with the film thickness. As the contrast of small islands was too low to measure with standard software for image analysis, the island size was measured on a video display by putting a proper semi-transparent ellipse which looked equivalent to each island.

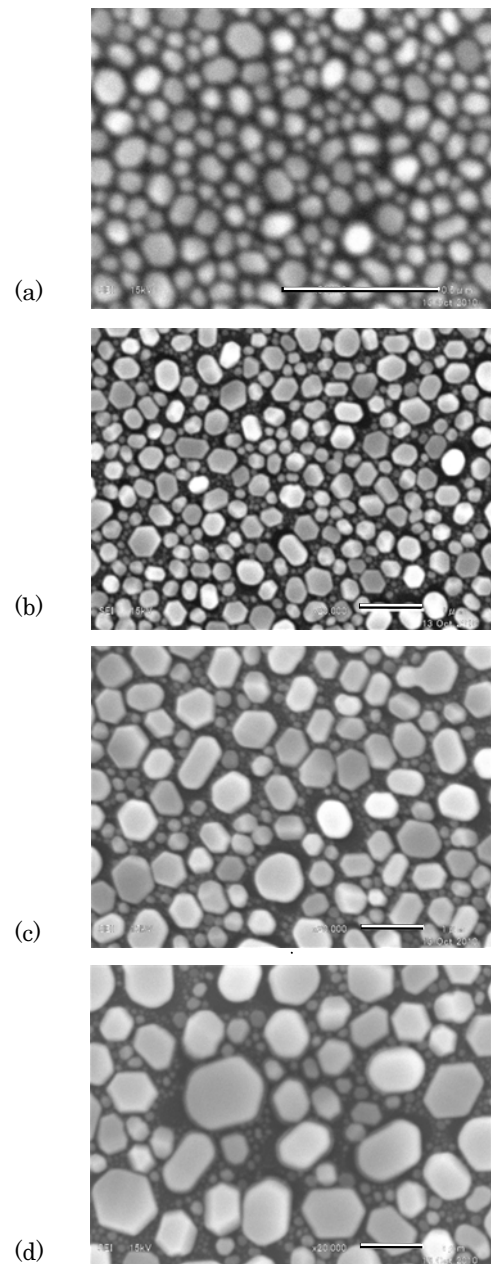


Fig.1 SEM images of indium films on Si(111). Mass thicknesses are (a) 30nm, (b) 60nm, (c) 90nm and (d) 120nm. The scale bar in each picture indicates  $1 \text{ } \mu\text{m}$ .

The elemental composition of In/Si(111) samples was measured in an XPS system (PHI model 1600), where the sample holder was cooled down to  $-100^{\circ}\text{C}$  in order to reduce the atomistic diffusion during the sputtering. Photoelectrons of the specimen excited by an X-ray of  $\text{MgK}\alpha$  (1253.6eV) were recorded with a concentric hemispherical energy analyzer (CHA). The sputter etching of the specimen was carried out by a focused energetic beam of  $\text{Ar}^+$  ions (3 keV, 2.3  $\mu\text{A}$ ) at an incidence angle of  $40^{\circ}$ . The ion beam was raster-scanned over the sample area of  $2\times 2\text{ mm}^2$ . A typical survey spectrum of the surface is given in Fig. 2. The depth-profiling that consisted of the sputter-etching for 10~30 s followed by an XPS measurement was automatically repeated for 60 minutes.

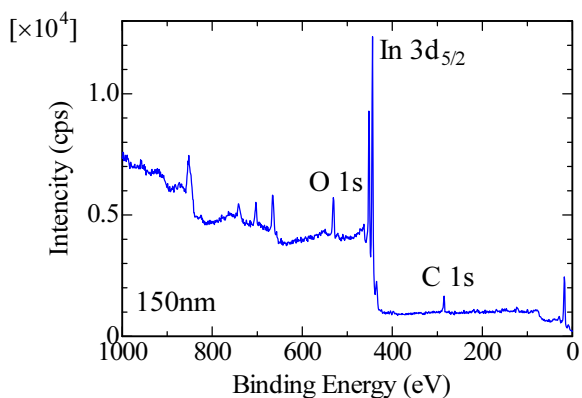


Fig.2 XPS survey spectrum obtained from a 150 nm-thick film of In on Si(111).

The photoelectron peaks of In, Si, C, and O were recorded at high resolution in the depth-profiling. The pressure during the depth-profiling was about  $10^{-6}$  Pa. We could determine the surface elemental composition by the following procedure. The spectral values, recorded at every 0.2 eV near the respective photoelectron peaks, were averaged by a 5-point smoothing of the Savitzky-Golay method, and the background signal created by using the Shirley method was subtracted as baseline<sup>12</sup>. Parameters of each element for the XPS analysis<sup>13</sup> are listed in Table I.

### 3. Results and Discussion

#### 3.1 Morphology of islands

Table I X-ray photoelectron peaks

Element	Orbit	Binding energy	Sensitivity factor
In	$3d_{5/2}$	443.9 eV	4.359
Si	2p	99.3 eV	0.339
C	1s	285 eV	0.296
O	1s	531 eV	0.711

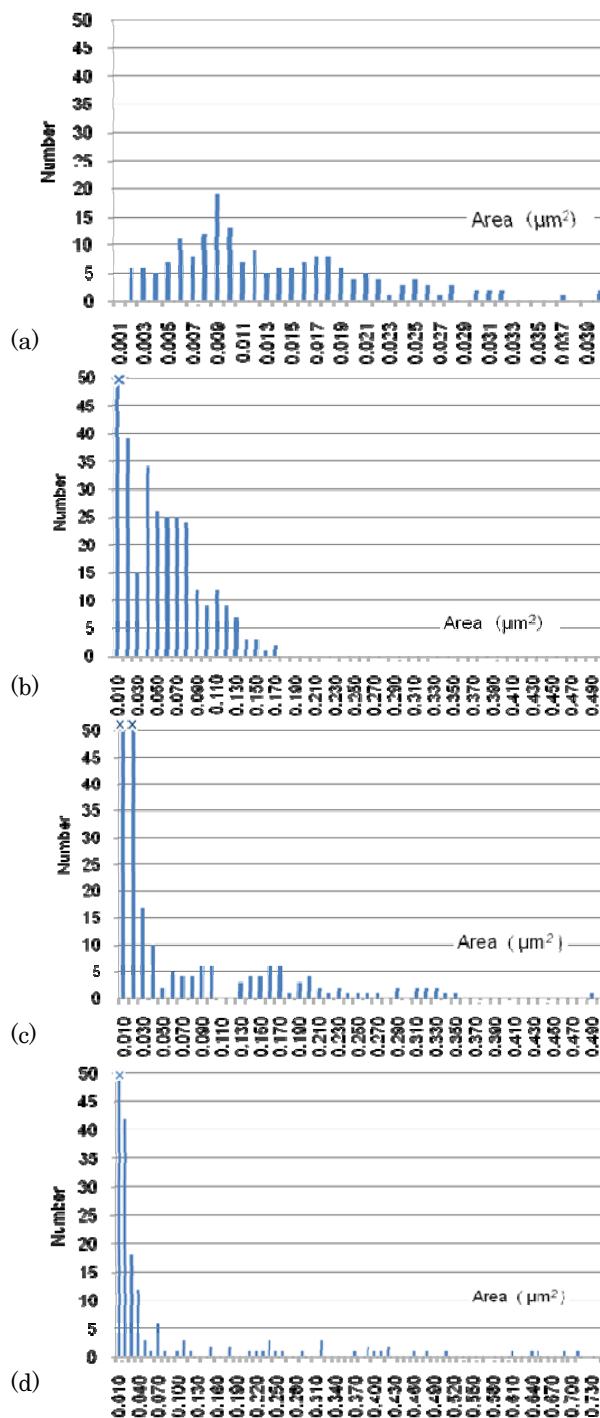


Fig. 3 Distribution of the projected area of islands whose film thicknesses are 30nm (a), 60nm (b), 90nm (c), and 120nm (d), respectively. The mark X on the column top denotes the scale overrun.

Areas containing 450~600 islands were examined in each SEM image of a different film thickness. The distributions are shown in Fig. 3 (a), (b), (c) and (d). Horizontal scale of Fig. 3 (a), (c) and (d) is taken so as to include the largest island. The evolution of island due to the deposition can be compared on the same scale between Fig. 3 (b) and (c). However, the growth can be demonstrated clearer if the distribution is expressed as a function of the island diameter.

As metal particles of nanometer size tend to have a liquid like nature, they become cap-shaped on the flat surface of solids. The volume  $V$  of a cap-shaped island, i.e., a truncated sphere, is geometrically given as a function of the contact area  $S$  and the Young's contact angle  $\theta$ .

$$V = \frac{S^{\frac{3}{2}}}{\alpha}, \quad \alpha = \frac{\pi^{\frac{1}{2}} \sin^3 \theta}{\frac{2}{3} - \cos \theta + \frac{1}{3} \cos^3 \theta}. \quad (1)$$

As the contact angle is determined by the nature of the contacting materials, the coefficient  $\alpha$  is constant for all islands. Measuring the contact area  $S_i$  of the  $i$ -th island and raising it to the 3/2 power, one can obtain a value of  $\alpha$  times the volume of the island  $V_i$ . In the present experiment where the deposited amount of the material is known as the film thickness, the coefficient  $\alpha$  can be determined by summing up  $S_i^{3/2}$  for all islands, and hence the contact angle  $\theta$  is calculated.

It should be noted that the SEM image of an island gives the maximum cross section of the island if the contact angle is greater than  $90^\circ$ . Then the surface area to volume ratio of Eq. (1) must be modified to Eq. (1') by employing a new coefficient  $\alpha'$  and the maximum cross section  $S'$ .

$$V = \frac{S'^{\frac{3}{2}}}{\alpha'}, \quad \alpha' = \frac{\pi^{\frac{1}{2}}}{\frac{2}{3} - \cos \theta + \frac{1}{3} \cos^3 \theta}. \quad (1')$$

In the experimental analysis, if the value of the contact angle calculated with Eq. (1) becomes greater than  $90^\circ$ , the true contact angle is obtained by a recalculation with Eq. (1'), where the sum of  $S_i^{3/2}$  corresponds to  $S_i'^{3/2}$ . Measured data of the sum of  $S_i$  and the calculated results are shown in Table II for different film thicknesses in the present experiment.

Alternatively the value of the sum of  $S_i^{3/2}$  divided by the surveyed area  $A$  is expected to be proportional to the

Table II Measured data of In islands on the Si surface.  $\alpha$ : film thickness,  $A$ : surveyed area,  $\alpha' = (\sum S_i^{3/2}) / (Ad)$

Thickness $d$ (nm)	$A$ ( $\mu\text{m}^2$ )	$\sum S_i$ ( $\mu\text{m}^2$ )	$\sum S_i^{3/2}$ ( $\mu\text{m}^3$ )	$\alpha$	$\theta$ (deg)
30	4.92	2.407	0.317	2.15	99
60	30.7	16.361	4.10	2.22	97
90	30.7	15.878	5.975	2.16	99
120	30.7	17.291	9.706	2.63	90

film thickness and is plotted against the film thickness in Fig. 4. One can see that the marked points for 30~90 nm-thick films are just on a straight line passing through the origin. This fact means that indium islands are similar in the shape for the thickness range from 30 to 90 nm. The slope gives a value of  $\alpha' = 2.17$ , which yields the contact angle of  $98 \pm 1^\circ$ . On the other hand the point for 120 nm thickness is about 25% above the straight line, and the contact angle was calculated to be about  $90^\circ$ . A greater value of  $\alpha'$  in the 120 nm-thick film means that islands are rather flat and that the coalescence cannot be completed like liquids when the film thickness exceeds 90 nm. Indium atoms cannot move over the size of an island, which is about  $1 \mu\text{m}$  in length at  $80^\circ\text{C}$ .

The contact angle of indium on silicon was rather great than that formed on the metal surface such as copper. The reason why the hydrophobic nature of the silicon surface appeared might be ascribed to the fact that the silicon surface was hydrogenated by the HF treatment to remove oxide layer.

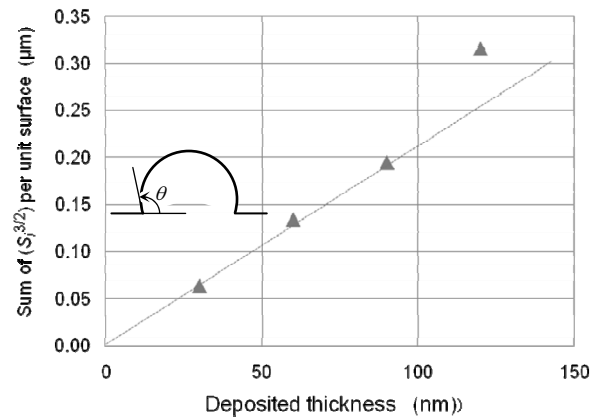


Fig. 4 Thickness dependence of  $(\sum S_i^{3/2})/A$  for islands of indium. The slope corresponds to  $\alpha$  or  $\alpha'$ . The cross section of an island in the linear region is illustrated as insert.

### 3.2 Depth-profiling of island structure

We have been studying the sputter-etching profile of island films, and have reported that the depth-profile curve of indium on silicon shows such a universal nature that all curves fall on a common curve when the sputter-etching time is normalized by the film thickness. In order to explain the behavior we have presented a structural model that the surface is covered almost completely with islands of the same size and that islands shrink at a rate proportional to the projected area of the island with keeping its shape.

It was observed that indium films were made up of hemispherical islands of a similar shape but the sizes were fairly distributed, as described above in Fig. 1 and 4. Therefore we started to investigate how the island shape and the size actually evolve along with the sputter-etching by the SEM observation.

Depth profiles of indium films of 30 nm and 120 nm thickness are shown in Fig. 5 (a) and (b), respectively. Horizontal axis is the sputtering time, and vertical axis is the surface composition. Contaminants of carbon and oxygen were observed at the top surface of the sample, but after 30~50 s of sputtering they disappeared. After that the elemental composition becomes only indium and silicon.

The surface composition of as-deposited samples, i.e. the value at  $t = 0$ , looks to come down from around unity in the lightly sputtered region, but we would like to make a point which has been reported in our previous study<sup>9,10</sup> that the decreasing curve of films is rather a quadratic function than an exponential decay if the film consists of islands of the same size. In Fig. 5 (a) and (b), the sputtering time is scaled in proportion to the film thickness, and we can see the universal nature that the curves (a) and (b) are almost the same.

### 3.3 Morphology of sputter-etched islands

In order to observe the change in the island structure, half-sputtered surfaces were prepared on each sample. They were not literally half but the sputtering periods were chosen so that the surface composition became roughly 0.71, 0.50 and 0.25, respectively ( Table III ).

Images of sputtered surfaces were also taken with SEM, and the distribution of island size was measured in

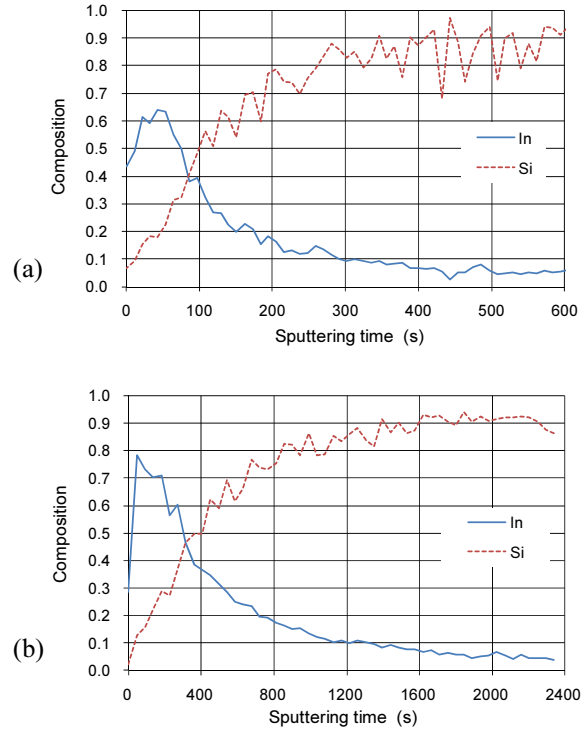


Fig. 5 XPS depth profiles of indium films on Si(111) surface. Initial thicknesses of indium are 30 nm (a) and 120 nm (b).

the same manner as described in the previous section. In order to get an overview of the sputtering process, we took some pictures of the sputtered surface. The sputtering proceeded in the order of images from (a) to (d) in Fig. 6, where indium was 60 nm thick. The pictures were taken from an oblique ( $45^\circ$ ) direction so as to capture the change intuitively not only in size but also in shape.

The pictures show that small islands disappear fast and that the shape does not change so much. The former behavior can be explained naturally by an assumption that the volume etching rate of an island is proportional to its projected area. If the following three

Table III Stepwise-sputtered samples of In

Thickness (nm)	Sputtering period (s)
30	(0), 30, 60, 120
60	(0), 60, 120, 240
90	(0), 90, 180, 360
120	(0), 120, 240, 480

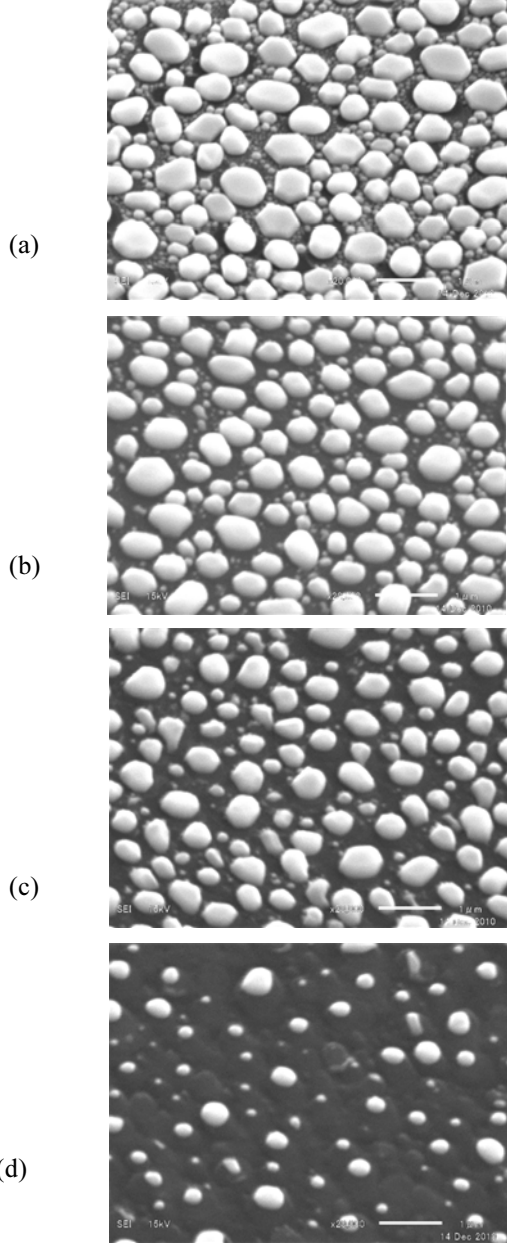


Fig. 6 Morphology change on the sputtered surface. Pictures were taken obliquely ( $45^\circ$ ) from the surface normal. The initial surface of 60 nm-thick film (a), etched for 60 s (b), for 120 s (c), and for 240 s (d), respectively. The mark bar indicates 1  $\mu$ m. They are not shot images from the same position.

relations are assumed between the parameters of the projected area  $S$ , apparent radius  $r$  and the volume  $V$ :

$$r \propto S^{\frac{1}{2}}; \quad V \propto S^{\frac{3}{2}}; \quad \frac{dV}{dt} \propto -S, \quad (2)$$

for an island, the time derivative of the radius and the area of an island can be expressed as:

$$\frac{dr}{dt} \propto \text{const.}, \quad \frac{dS}{dt} \propto -r \quad (< 0). \quad (3)$$

Smaller islands disappear more promptly, and the signal contribution by smaller islands becomes less because the decreasing rate,  $(dS/dt)/S$ , is negatively greater for smaller islands. That is, smaller islands do not play a dominant role in the derivative behavior and the gross change is controlled only by large islands.

The analysis mentioned in 3.1 was applied to the SEM images of the sputter-etched surface, and the distribution of islands was obtained. The measured surface coverage of islands, i.e.,  $(\sum S_i)/A$  as given in Table II, was compared with the composition of indium measured from the depth profile data of the XPS. For as-deposited samples composition of indium was estimated by extrapolating the data in the range where contaminants disappeared. The extrapolated values were  $1.02 \pm 0.05$ , which are given in the parenthesis in Fig. 7. It is found that the apparent coverage of island on the surface is as low as a half of the surface elemental composition. That the elemental composition is higher than the areal ratio means a good amount of indium are scattered on the flat area on the surface. Though the solubility of indium in silicon is very low ( $8 \times 10^{-4}$  at.%), it is well known that indium atoms have a strong interaction with silicon atoms on the surface and some atoms are extremely mobile on the silicon surface.<sup>14-18</sup> In an experiment on indium-implanted silicon surface, a complex segregation behavior<sup>19</sup> has

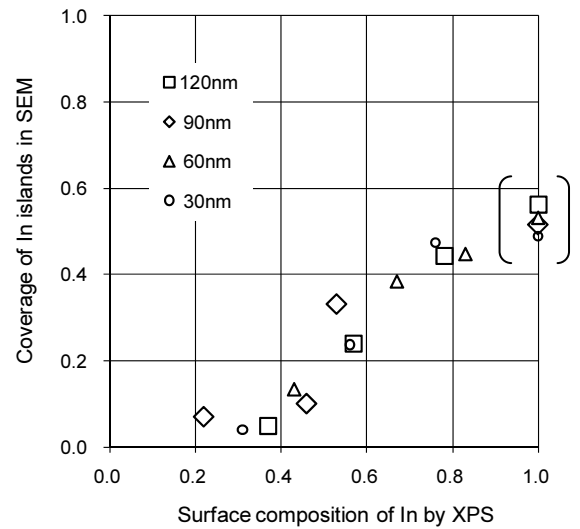


Fig. 7 Comparison of the surface coverage of indium islands in the SEM image with the composition measured from XPS measurement. Values of the surface composition 1.0 in XPS measurements were those extrapolated.

been observed, where it is ascribed to an activated surface condition.

#### 4. Conclusion

The size distribution of indium islands on Si(111) surface and the morphology change caused by sputter-etching have been studied with the secondary electron microscope and the X-ray photoelectron spectroscopy. The XPS signal of indium showed that the surface of silicon was totally covered with indium. However, about only 50% of the surface was found to be covered with islands. Islands could be assumed to have a hemispherical shape with a contact angle of  $98^\circ$  for the thickness range from 30 to 90 nm, and islands could coalesce completely to form a large one after they contacted each other. For films thicker than 120 nm, the surface area to volume ratio became great and the coalescence was incomplete. When islands were sputtered, the area of islands and the XPS signal decreased and islands shrank in size while keeping the shape similar. However, the magnitude of the XPS signal of indium, which was about twice as much as the coverage of islands, suggested indium atoms were dispersed on the flat area between islands.

#### Acknowledgement

This work has been financially supported by the Special Funds of Seikei University, Science and Technology.

#### References

- 1) U. Diebold, J-M. Pan, and T.E. Madey: Surface Sci., **331-333**, Part 2 (1995) pp. 845-854.
- 2) H.J. Scheel: Control of Epitaxial Growth Modes for High-Performance Devices, in “*Crystal Growth Technology*” (eds H. J. Scheel and T. Fukuda), ch. 28,

John Wiley & Sons (Chichester, 2004).

- 3) T. Nakano, T. Suzuki, N. Ohnuki and S. Baba: Thin Solid Films, **334** (1998) pp. 192-195.
- 4) T. Nakano, H. Mizuhashi and S. Baba : Jpn. J. Appl. Phys., **44** (2005) pp. 1932-1938.
- 5) G.E. Rhead, M-G. Barthes and C. Argile: Thin Solid Films, **82**(2) (1981) pp. 201-211.
- 6) C. Argile and G. E. Rhead: Surface Sci. Reports, **10** (1989) 277.
- 7) M. Tomellini and G.A. Attard: Surface Sci., **245** (3) (1991) pp. L179-L184.
- 8) C.W. Magee and R.E. Honig: Surface and Interface Analysis, **4** (1982) pp. 35-41.
- 9) T. Nakano, S. Sato and S. Baba: Vacuum, **74** (2004) pp. 591-594.
- 10) S. Sato, T. Nakano, S. Baba: Shinku (J. Vac. Soc. Jpn.) **48** (2005) pp. 121-124 in Japanese.
- 11) R.W. Olesinski, N. Kanani, and G.J. Abbaschian: Bulletin of Alloy Phase Diagram, **6** (1985) 128.
- 12) D. Briggs and M.P. Seah ed.: “*Practical Surface Analysis by Auger and X-ray Photoelectron Spectroscopy*” (Wiley, Sussex, 1983 ).
- 13) K. Chastain: “*Handbook of Electron Spectroscopy*” (Perkin-Elmer Corp., Minnesota, 1992) Appendix F.
- 14) I. C. Kizilyalli, T. L. Rich, F. A. Stevie, and C. S. Rafferty :J. Appl. Phys. **80** (1996) pp. 4944-4947.
- 15) J.M. Zhou, a, S. Baba and A. Kinbara: Thin Solid Films, **98** (1982) pp. 109-113.
- 16) S. Solmi, A. Parisini, M. Bersani, D. Giubertoni, V. Soncini, G. Carnevale, A. Benvenuti, and A. Marmioli:J. Appl. Phys. **92** (2002) pp.1361-1366.
- 17) T. Noda: J. Appl. Phys. **91** (2002) pp. 639-645.
- 18) C.E. Allen, R. Ditchfield, E.G. Seebauer: J. Vac. Sci. Technol. A, **14** (1996) pp. 22- 29.
- 19) P. Baeri, J. M. Poate, S. U. Campisano, G. Foti, E. Rimini, A. G. Cullis: Appl. Phys. Lett., **37** (1980) pp. 912-914.

---

#### Appendix 1: A universal nature observed in depth profiles for films of island structure

When vapor atoms fall on a solid surface, they once adhere to the surface weakly and migrate around until

they become nuclei of condensed phase or they are captured by other established solid structure. As the deposited atoms are mobile and the interaction is isotropic, they form spherical islands truncated at the substrate surface. The islands behave like liquid drops

to form a large island when they touch each other physically. When the deposition is stopped, atoms are finalized to realize the lowest free energy condition.

Now a cap-shaped island (the volume  $V$  and the projected area  $S$ ) is formed on a flat surface. The shape of an island is only characterized by its contact angle  $\theta$  in a condensate(c)-vapor(v)-substrate(s) system, which is determined by Young's equation for the minimization of the surface free energies

$$\sigma_{cv} \cos \theta = \sigma_{sv} - \sigma_{sc} \quad (\text{A1})$$

Here,  $\sigma$  denotes the interfacial free energy and the suffixes  $cv$ ,  $sv$  and  $sc$  denote the contacting two phases in the system. The volume of an island  $V$  has a geometrical relation to the contact area  $S$  as

$$V = \frac{S^{\frac{3}{2}}}{\alpha}, \quad \alpha = \frac{\pi^2 \sin^3 \theta}{\frac{2}{3} - \cos \theta + \frac{1}{3} \cos^3 \theta}. \quad (\text{A2})$$

Below is given how an island shrinks in size with the sputtering time. The sputtering removes the surface atoms at a rate proportional to the flux of the energetic beam and the sputtering yield of the material. Then the volume reduction rate of an island is given as

$$\frac{dV}{dt} = -\eta S \quad (\text{A3})$$

where  $\eta$  is the ejection flux per unit projected area of the island. Substituting  $V$  with  $S$  in eq.(A2), one can get a rate equation for  $S$  and the solution for  $S$  is obtained as a quadratic function of  $t$ :

$$\frac{dS}{dt} = -\frac{2}{3} \alpha \eta S^{\frac{1}{2}} \quad (\text{A4})$$

$$S(t) = S_0 \left( 1 - \frac{\alpha \eta}{3 S_0^{\frac{1}{2}}} t \right)^2 \quad (\text{A5})$$

where  $S_0$  is the projected area of the island at  $t = 0$ .

Here we assume that the surface is covered with islands of the same size and the areal density of island is  $n$ . The assumption is too simple but the small islands disappear very rapidly as mentioned in the body part. Then the initial surface coverage  $\theta_0$  and the film thickness  $d$  are given respectively as

$$\theta_0 = n \cdot S_0, \quad d = n \cdot V_0 \quad (\text{A6})$$

Finally the coverage change due to the sputtering is obtained as a form of

$$\frac{\theta(t)}{\theta_0} \equiv \frac{n \cdot S_i(t)}{\theta_0} = \left\{ 1 - \frac{\eta}{3} \left( \frac{\theta_0 \cdot t}{d} \right) \right\}^2 \quad (\text{A7})$$

It should be noted that this formula does not contain any shape parameters such as  $\theta$  and hence the coverage change shows a universal nature as a function of  $(t/d)$ . This characteristic nature suggests an experimental method to study the nature of sputtering, because one can obtain values of the sputtering yield, which vary with ion energy and the incidence angle, only by measuring a depth profile for island films.

## Appendix 2: Sputtering yields by depth-profiling

The method has been applied to the sputtering experiment of indium films on Si(111). Depth profiles such as shown in Fig.5 were analyzed using the eq. (A7). Here, the initial coverage was taken  $\theta_0 = 1$ . Results of values of the removal rate  $\eta$  are shown in Fig. A1. A value of  $\eta = 0.34 \pm 0.02$  nm/s was obtained in the thickness range between 30 and 90 nm, where the island shape was similar, and it was slightly greater than those obtained from the thicker region.

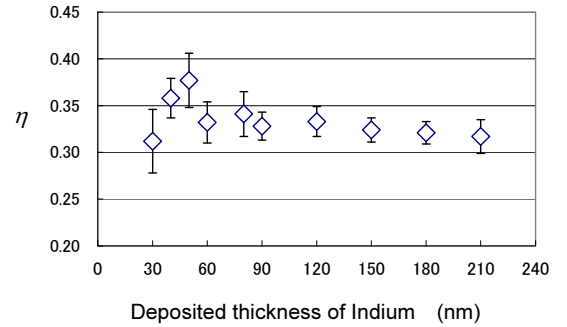


Fig. A1 Atomic removal rate  $\eta$  in eq. (A3) obtained from the curve-fitting to the depth-profile data. Data of 30 nm and 120 nm correspond to those shown in Fig.7.

As the sputtering yield  $\gamma$  is defined as the ratio of ejected atoms to the incident atoms it is calculated from the formula

$$\gamma = \frac{\eta \cdot \rho \cdot e}{j} \quad (\text{A8})$$

where  $j$  is the current density of the single-charged ion beam and  $\rho$  the number density of atoms per volume. Values of  $\eta = 0.34$  nm/s,  $\rho = 3.83 \times 10^{28}$  atoms/m<sup>3</sup>,  $j = 0.58$  A/m<sup>2</sup> result in a sputtering yield of  $\gamma = 3.6 \pm 0.2$ , where the literature data for 3 keV Ar<sup>+</sup> ions is  $\gamma = 2.9$ .<sup>†</sup>

<sup>†</sup> [ K. Kanaya, K. Hojo, K. Koga and K. Toki: Jpn. J. Appl. Phys. **12** (1973) 1297 ]